

## Ion Solvation Thermodynamics from Simulation with a Polarizable Force Field

Alan Grossfield, Pengyu Ren, and Jay W. Ponder\*

Contribution from the Department of Biochemistry and Molecular Biophysics, Washington University School of Medicine, 660 South Euclid Avenue, Saint Louis, Missouri 63110

Received July 1, 2003; E-mail: ponder@dasher.wustl.edu

**Abstract:** Thermodynamic measurements of the solvation of salts and electrolytes are relatively straightforward, but it is not possible to separate total solvation free energies into distinct cation and anion contributions without reference to an additional extrathermodynamic assumption. The present work attempts to resolve this difficulty using molecular dynamics simulations with the AMOEBA polarizable force field and perturbation techniques to directly compute absolute solvation free energies for potassium, sodium, and chloride ions in liquid water and formamide. Corresponding calculations are also performed with two widely used nonpolarizable force fields. The simulations with the polarizable force field accurately reproduce in vacuo quantum mechanical results, experimental ion–cluster solvation enthalpies, and experimental solvation free energies for whole salts, while the other force fields do not. The results indicate that calculations with a polarizable force field can capture the thermodynamics of ion solvation and that the solvation free energies of the individual ions differ by several kilocalories from commonly cited values.

### 1. Introduction

The presence, type, and concentration of salt can dramatically alter the solubility and behavior of other molecules in solution. As a result, ion solvation is important to many topics of chemical interest, including surface chemistry, environmental chemistry, and the study of molecules such as surfactants, colloids, and polyelectrolytes. Biologically, ions are critical to the structure and function of nucleic acids, proteins, and lipid membranes.<sup>1</sup> Ions interact with biomolecules in a variety of ways: nonspecifically as in counterion condensation around nucleic acids, binding to specific sites for purposes of stabilization and catalysis as in many proteins, or at a distance by modifying the electrostatic properties of the solution.

Ions also act as signaling molecules, especially when transferred across membranes by ion channels.<sup>2</sup> The experimental crystal structures of several ion channels have been published in recent years.<sup>3–5</sup> The two potassium channel structures revealed that their selectivity for K<sup>+</sup> over other cations is mediated by ion–backbone interactions. Upon entering the channel, K<sup>+</sup> exchanges water for coordination by backbone carbonyl oxygens with little or no free energy barrier. As a result, K<sup>+</sup> permeates the channel very quickly, almost at the diffusion limit.<sup>2,3</sup> Other ions such as Na<sup>+</sup> face significant barriers, because their permeability is very small.

Ion channels are only one of many important chemical systems involving ion transfer between phases. For example, the transfer of ions between media obviously plays a critical role in the design of effective ion-exchange resins, used in chemical purification.<sup>6</sup> A detailed understanding of the interactions of ions in solution is a major contributor to the understanding of selectivity and separation in chromatographic systems.<sup>7</sup> A great deal of work has been done investigating the binding of alkali metal cations to crown ethers.<sup>8</sup>

Ionic solvation thermodynamics are also of interest in the calibration of general theories of solvation. Many authors have used this information in developing continuum solvation models; a common approach is to start with the Born equation<sup>9</sup> and modify it to improve its quantitative accuracy.<sup>10–18</sup> Similarly, the parameters used to perform molecular simulations involving simple ions are typically derived by fitting to this type of data.<sup>19</sup>

In many cases, the quantity of greatest interest is the free energy of solvation or transfer for a specific ionic species. However, this value cannot be derived directly from experiment. At equilibrium, bulk solutions are electrically neutral, meaning that a transferred cation must be accompanied by a neutralizing

- (1) Tieleman, D. P.; Biggin, P. C.; Smith, G. R.; Sansom, M. S. P. *Q. Rev. Biophys.* **2001**, *34*, 473.
- (2) Hille, B. *Ionic Channels of Excitable Membranes*, 3rd ed.; Sinauer Associates, Inc.: Sunderland, MA, 2001.
- (3) Doyle, D. A.; Cabral, J. M.; Pfuetzner, R. A.; Kuo, A. L.; Gulbis, J. M.; Cohen, S. L.; Chait, B. T.; MacKinnon, R. *Science* **1998**, *280*, 69.
- (4) Jiang, Y. X.; Lee, A.; Chen, J. Y.; Ruta, V.; Cadene, M.; Chait, B. T.; MacKinnon, R. *Nature* **2003**, *423*, 33.
- (5) Dutzler, R.; Campbell, E. B.; Cadene, M.; Chait, B. T.; MacKinnon, R. *Nature* **2002**, *415*, 287.

- (6) Okada, T. *J. Chem. Soc., Faraday Trans.* **1991**, 3027.
- (7) Okada, T. *Anal. Sci.* **1998**, *14*, 469.
- (8) Takeda, Y.; Kanazawa, M.; Katsuta, S. *Anal. Sci.* **2000**, 929.
- (9) Born, M. *Z. Phys.* **1920**, *1*, 45.
- (10) Latimer, W. M.; Pitzer, K. S.; Slansky, C. M. *J. Chem. Phys.* **1939**, *7*, 108.
- (11) Rashin, A. A.; Honig, B. *J. Phys. Chem.* **1985**, *89*, 5588.
- (12) Abe, T. *J. Phys. Chem.* **1986**, *90*, 713.
- (13) Roux, B.; Yu, H. A.; Karplus, M. *J. Phys. Chem.* **1990**, *94*, 4683.
- (14) Chan, S. L.; Lim, C. *J. Phys. Chem.* **1994**, *98*, 692.
- (15) Hyun, J.; Ichiye, T. *J. Chem. Phys.* **1998**, *109*, 1074.
- (16) Kumar, A. *J. Phys. Soc. Jpn.* **1992**, 4247.
- (17) Badarayani, R.; Kumar, A. *Indian J. Chem., Sect. A* **2000**, *39*, 584.
- (18) Babu, C. S.; Lim, C. *J. Phys. Chem. A* **2001**, *105*, 5030.
- (19) Åqvist, J. *J. Phys. Chem.* **1990**, *94*, 8021.

anion, and vice versa. So, while the solvation free energy for a salt can be measured, it is impossible to separate it experimentally into contributions from the cation and anion.<sup>20–22</sup> Rather, an additional extrathermodynamic assumption is required to perform this dissection.<sup>23,24</sup>

There are at least four different kinds of model assumptions in use. In the first approach, a reference salt is proposed, where it is assumed that the cation and anion have identical solvation thermodynamics in all solvents. The free energy, enthalpy, and entropy of solvation for the reference salt can then be equally divided between its component species. Once the absolute solvation energies of the reference cation and anion are known, they provide a standard against which to measure the relative thermodynamics of other ions.

The most common choice as a reference salt is tetraphenylarsonium tetraphenylborate ( $\text{Ph}_4\text{As}^+\text{Ph}_4\text{B}^-$  or TATB),<sup>21,25–27</sup> although tetraphenylphosphonium tetraphenylborate ( $\text{Ph}_4\text{P}^+\text{Ph}_4\text{B}^-$  or TPTB) is also used.<sup>22</sup> The assumption is that the tetraphenyl ions are sufficiently large and hydrophobic that there are no charge-specific solvent ordering effects, leaving only Born-like dielectric solvation, which is independent of the sign of the charge.

While the TATB assumption cannot be directly verified or falsified experimentally, there is a significant amount of indirect evidence that it does not accurately describe solvation in water. Differential near-infrared spectroscopy indicates that  $\text{Ph}_4\text{As}^+$  and  $\text{Ph}_4\text{B}^-$  have qualitatively different effects on water structure;<sup>28</sup> the anion acts as a structure breaker, while the cation has little specific effect. Stangret and Kamińska-Piotrowicz used FTIR spectroscopy in HDO and  $\text{H}_2\text{O}$  to conclude that the anion significantly diminishes the hydrogen bond energy of water.<sup>29</sup> More recent work from the same group confirmed this conclusion and argued that anions in general are better solvated than cations.<sup>30</sup> Proton NMR experiments have shown that  $\text{Ph}_4\text{P}^+$  and  $\text{Ph}_4\text{As}^+$  cause an upfield chemical shift of the water proton, while  $\text{Ph}_4\text{B}^-$  causes a downfield shift, again demonstrating sign-specific effects on water structure.<sup>31</sup> Analogous phenomena have been seen in other organic solvents, indicating the TATB assumption is likely flawed in these solvents as well, and most especially when applied to transfer between solvents. Cyclic voltammetry experiments have also been used to indict the TATB assumption.<sup>32</sup>

Moreover, several groups have argued against the TATB assumption through use of computational methods. Schurhammer and Wipff have performed molecular dynamics simulations of  $\text{Ph}_4\text{As}^+$  and  $\text{Ph}_4\text{B}^-$  in water which indicate the anion solvation free energy is significantly lower than that of the cation.<sup>33–35</sup>

Quantum calculations using continuum solvent models have been used to draw similar conclusions.<sup>36,37</sup>

The second extrathermodynamic assumption in common use involves the estimation of proton solvation as the benchmark. This approach is also problematic. For example, Schmid et al.<sup>38</sup> assume that the solvation entropies of  $\text{H}^+$  and  $\text{OH}^-$  in water are equal and use the self-consistent analysis of Krestov<sup>39</sup> to derive the hydration enthalpy of the proton. The proton thermodynamics can then be used to set the scale for other ions. To our knowledge, no equivalent analysis has been performed for solvents other than water, limiting the generality of this approach. Moreover, there is significant controversy regarding the correct solvation entropy for the proton.<sup>40,41</sup>

The third approach was suggested by Latimer et al.<sup>10</sup> They used the Born equation with the additional assumption that the effective ionic radii in solution could be derived from the corresponding crystal radii incremented by a constant. Two separate constants were chosen for cations and anions to match experimental differences in the solvation free energies of ions of like sign. Once the ionic radii were determined, the experimental salt solvation free energies were separated into individual cation and anion contributions such that ions of both signs obey the Born equation. This procedure has the advantage that it avoids the use of a reference salt. However, the data show a systematic deviation from the Born equation, and the constants must be refit for each solvent of interest.

The fourth approach is the cluster pair approximation, described by Tissandier et al.<sup>42</sup> and further elaborated by Tuttle, Jr. et al.<sup>43</sup> This method combines experimental free energies of small ion–water clusters with free energies of solvation for cations and anions relative to  $\text{H}^+$  and  $\text{OH}^-$ , respectively, to estimate the free energy of hydration for the proton. Once this value is set, the other absolute free energies of hydration are determined. While the authors explicitly state that this method involves no extrathermodynamic assumptions, this is not in fact the case. Rather, their analysis depends on the assumption that, in the limit of a large ion–water cluster, the free energy of solvation does not depend on the sign of the ion charge (see eq 9 of ref 42). Moreover, creating a spherical cavity in water generates a positive electrostatic potential at the center.<sup>44</sup> This potential does not go to zero as the cavity becomes infinitely large.<sup>45</sup> As a result, the solvation free energies for even infinitely large cation–water and anion–water clusters should differ.

Molecular simulation would appear to be an ideal way to resolve the difficulties outlined above, because one can directly simulate a single cation or anion in any solvent. To perform

- (20) Rosseinsky, D. R. *Chem. Rev.* **1965**, *65*, 467.  
(21) Marcus, Y. *J. Chem. Soc., Faraday Trans.* **1986**, *82*, 233.  
(22) Kalidas, C.; Hefter, G.; Marcus, Y. *Chem. Rev.* **2000**, *100*, 819.  
(23) Grunwald, E.; Baughman, G.; Kohnstam, G. *J. Am. Chem. Soc.* **1960**, *82*, 5801.  
(24) Friedman, H. L.; Krishnan, C. V. *Thermodynamics of Ion Hydration. In Water: A Comprehensive Treatise*; Franks, F., Ed.; Plenum Press: New York, 1973; Vol. 3.  
(25) Cox, B. G.; Parker, A. J. *J. Am. Chem. Soc.* **1973**, *95*, 402.  
(26) Marcus, Y. *J. Chem. Soc., Faraday Trans. 1* **1987**, *83*, 339.  
(27) Marcus, Y. *J. Chem. Soc., Faraday Trans. 1* **1987**, *83*, 2985.  
(28) Jolicœur, C.; Dinh The, N.; Cabana, A. *Can. J. Chem.* **1971**, *49*, 2008.  
(29) Stangret, J.; Kamińska-Piotrowicz, E. *J. Chem. Soc., Faraday Trans.* **1997**, *93*, 3463.  
(30) Stangret, J.; Gampe, T. *J. Phys. Chem. A* **2002**, *106*, 5393.  
(31) Coetzee, J. F.; Sharpe, W. R. *J. Phys. Chem.* **1971**, *75*, 3141.  
(32) Shao, Y.; Stewart, A. A.; Girault, H. H. *J. Chem. Soc., Faraday Trans.* **1991**, *87*, 2593.

- (33) Schurhammer, R.; Wipff, G. *J. Phys. Chem. A* **2000**, *104*, 11159.  
(34) Schurhammer, R.; Wipff, G. *J. Mol. Struct.* **2000**, *500*, 139.  
(35) Schurhammer, R.; Engler, E.; Wipff, G. *J. Phys. Chem. B* **2001**, *105*, 10700.  
(36) Luzhkov, V.; Warshel, A. *J. Comput. Chem.* **1992**, *13*, 199.  
(37) Schamberger, J.; Clarke, R. *J. Biophys. J.* **2002**, *82*, 3081.  
(38) Schmid, R.; Miah, A. M.; Sapunov, V. *N. Phys. Chem. Phys.* **2000**, *2*, 97.  
(39) Krestov, G. A. *Thermodynamics of Solvation: Solution and Dissolution, Ions and Solvents, Structure and Energetics*; Ellis Horwood Ltd.: New York, 1991.  
(40) Conway, B. E. *J. Solution Chem.* **1978**, *7*, 721.  
(41) Goodrich, J. C.; Goyan, F. M.; Morse, E. E.; Preston, R. G.; Young, M. B. *J. Am. Chem. Soc.* **1950**, *72*, 4411.  
(42) Tissandier, M. D.; Cowen, K. A.; Feng, W. Y.; Gundlach, E.; Cohen, M. H.; Earhart, A. D.; Coe, J. V.; Tuttle, T. R., Jr. *J. Phys. Chem. A* **1998**, *102*, 7787.  
(43) Tuttle, T. R., Jr.; Malaxos, S.; Coe, J. V. *J. Phys. Chem. A* **2002**, *106*, 925.  
(44) Ashbaugh, H. S. *J. Phys. Chem. B* **2000**, *104*, 7235.  
(45) Asthagiri, D.; Pratt, L. R.; Ashbaugh, H. S. *J. Chem. Phys.* **2003**, *119*, 2702.

simulations of a solvated ion, it is necessary to assign repulsion–dispersion (“van der Waals”) parameters to the ion. However, these ion parameters are generally fit to match chosen “experimental” ion solvation free energies.<sup>19</sup> In addition, the traditional van der Waals size and well-depth parameters are not uniquely determined by just the solvation free energy. There is in some sense only a single independent quantity, the effective radius of the ion, which can be reproduced by a broad range of parameters.

High-level quantum mechanical calculations have been performed on ion–water dimers<sup>46,47</sup> and could be used to choose ion parameters. Unfortunately, standard pairwise molecular force fields cannot simultaneously reproduce in vacuo microscopic and bulk properties with the same parameters, because the effects of electronic polarization must be included implicitly. Similarly, parameters appropriate for solvation by one solvent may not be appropriate for another. This kind of transferability can be critical in the simulation of systems of biophysical interest. For example, Roux and co-workers state that their simulations of potassium permeation of the KcsA channel did not produce reasonable results until separate van der Waals parameters were used to describe K<sup>+</sup>–water and K<sup>+</sup>–protein interactions.<sup>48,49</sup> The K<sup>+</sup>–protein parameters were chosen to alter the transfer free energy for potassium between water and *N*-methylacetamide (NMA), with the latter chosen as a model for the peptide backbone.

One approach which has met with some success recently is to perform simulations mixing quantum mechanical and classical potentials. For example, Tongraar and Rode used QM/MM molecular dynamics to examine the water structure around fluoride and chloride anions.<sup>50</sup> Unfortunately, such calculations are restricted to small systems and relatively short trajectories, because quantum calculations are far more expensive than molecular mechanics. An alternative, less costly method is to use a quasi-chemical approximation, where the ion and first shell of waters are held rigid and treated quantum mechanically while the surrounding medium is treated using either classical molecular dynamics or continuum theory.<sup>45,51–54</sup> This approach is far less expensive than standard QM/MM methods, while retaining much of the accuracy of the quantum calculations in the region immediately surrounding the ion. However, it is not easily applied to systems where the first solvation shell is relatively unstructured or heterogeneous. Further, such methods cannot be used directly to treat multiple environments encountered during a single simulation, as when an ion enters an ion channel.

Similarly, several groups have performed molecular dynamics simulations of ions using polarizable force fields. One of the earliest studies included a rough estimate of the hydration enthalpy for several ions.<sup>55</sup> Multiple groups have employed

polarizable force fields to investigate the properties of small chloride–water clusters, where polarization appears essential to reproduce the correct cluster geometry.<sup>56–59</sup> More recently, Dang and co-workers have performed extensive simulations of ion binding to liquid–vapor interfaces,<sup>60,61</sup> with emphasis on the thermodynamic preference of halide anions for the interfacial region. Jungwirth and Tobias have used a combination of quantum molecular dynamics and classical dynamics with polarizable force fields to investigate the location of various ions in water slabs as a function of ion concentration.<sup>62,63</sup> Carrillo-Tripp et al.<sup>64</sup> extended their polarizable MDCHO water model to a comparison of the solvation of Na<sup>+</sup> and K<sup>+</sup> in water. However, none of these works report solvation free energies for the ions.

The present effort describes the application of the newly developed AMOEBA (Atomic Multipole Optimized Energetics for Biomolecular Applications) polarizable force field to the calculation of ionic solvation free energies. Specifically, van der Waals parameters are chosen for potassium, sodium, and chloride, using high-level quantum mechanics and experimental cluster hydration enthalpies, combined with solvent parameters determined previously using neat liquid and gas-phase cluster simulations.<sup>65</sup> These parameters are then used to compute the solvation free energy for each ion in two solvents, water and formamide, using molecular dynamics and free energy perturbation. In addition to the AMOEBA force field, calculations were performed with CHARMM27<sup>66</sup> and OPLS-AA,<sup>67</sup> two commonly used nonpolarizable force fields. The calculations with the AMOEBA force field accurately reproduce a range of experimental solvation free energies. Consequently, we argue that these simulations can provide definitive cation and anion solvation free energies, without reference to extrathermodynamic constraints such as the TATB assumption.

## 2. Methods

**2.1. Force Field Parameters.** Three sets of force field parameters were compared: OPLS-AA, CHARMM27, and AMOEBA. The OPLS-AA computations were performed using the ion parameters of Åqvist,<sup>19</sup> in combination with the TIP3P water model<sup>68</sup> and the OPLS-AA parameters<sup>67</sup> for NMA. Because the original OPLS-AA parametrization does not contain formamide values, we chose parameters consistent with those published for acetamide and *N*-methylformamide.<sup>67</sup> In passing, it should be noted that OPLS-AA also defines a second set of sodium parameters,<sup>69</sup> intended for use with the TIP4P water model, which were not considered in this work. The CHARMM27 simulations were performed with the ion parameters from the most recently released

- (46) Feller, D.; Glendening, E. D.; Woon, D. E.; Feyereisen, M. W. *J. Chem. Phys.* **1995**, *103*, 3526.  
(47) Xantheas, S. S. *J. Phys. Chem.* **1996**, *100*, 9703.  
(48) Roux, B.; Bernèche, S. *Biophys. J.* **2002**, *82*, 1681.  
(49) Bernèche, S.; Roux, B. *Nature* **2001**, *414*, 73.  
(50) Tongraar, A.; Rode, B. M. *Phys. Chem. Chem. Phys.* **2003**, *5*, 357.  
(51) Tawa, G. J.; Topol, I. A.; Burt, S. K.; Caldwell, R. A.; Rashin, A. A. *J. Chem. Phys.* **1998**, *109*, 4852.  
(52) Zhan, C.-G.; Dixon, D. A. *J. Phys. Chem. A* **2001**, *105*, 11534.  
(53) Zhan, C.-G.; Dixon, D. A. *J. Phys. Chem. A* **2002**, *106*, 9737.  
(54) Grabowski, P.; Riccardi, D.; Gomez, M. A.; Asthagiri, D.; Pratt, L. R. *J. Phys. Chem. A* **2002**, *106*, 9145.  
(55) Lybrand, T. P.; Kollman, P. A. *J. Chem. Phys.* **1985**, *83*, 2923.  
(56) Stuart, S. J.; Berne, B. J. *J. Phys. Chem.* **1996**, *100*, 11934.

- (57) Perera, L.; Berkowitz, M. L. *J. Chem. Phys.* **1991**, *95*, 1954.  
(58) Perera, L.; Berkowitz, M. L. *J. Chem. Phys.* **1993**, *99*, 4236.  
(59) Perera, L.; Berkowitz, M. L. *J. Chem. Phys.* **1994**, *100*, 3085.  
(60) Dang, L. X.; Chang, T.-M. *J. Phys. Chem. B* **2002**, *106*, 235.  
(61) Dang, L. X. *J. Phys. Chem. B* **2002**, *106*, 10388.  
(62) Jungwirth, P.; Tobias, D. J. *J. Phys. Chem. B* **2001**, *105*, 10468.  
(63) Jungwirth, P.; Tobias, D. J. *J. Phys. Chem. B* **2002**, *106*, 6361.  
(64) Carrillo-Tripp, M.; Saint-Martin, H.; Ortega-Blake, I. *J. Chem. Phys.* **2003**, *118*, 7062.  
(65) Ren, P.; Ponder, J. W. *J. Phys. Chem. B* **2003**, *107*, 5933.  
(66) MacKerell, A. D., Jr.; Bashford, D.; Bellott, M.; Dunbrack, R. L., Jr.; Evanseck, J. D.; Field, M. J.; Fischer, S.; Gao, J.; Guo, H.; Ha, S.; Joseph-McCarthy, D.; Kuchnir, L.; Kuczera, K.; Lau, F. T. K.; Mattos, C.; Michnick, S.; Ngo, T.; Nguyen, D. T.; Prodhom, B.; Reiher, W. E., III; Roux, B.; Schlenkrich, M.; Smith, J. C.; Stote, R.; Straub, J.; Watanabe, M.; Wiorkiewicz-Kuczera, J.; Yin, D.; Karplus, M. *J. Phys. Chem. B* **1998**, *102*, 3586.  
(67) Jorgensen, W. L.; Maxwell, D. S.; Tirado-Rives, J. *J. Am. Chem. Soc.* **1996**, *118*, 11225.  
(68) Jorgensen, W. L.; Chandrasekhar, J.; Madura, J. D.; Impey, R. W.; Klein, M. L. *J. Chem. Phys.* **1983**, *79*, 926.  
(69) Jorgensen, W. L.; Severance, D. L. *J. Chem. Phys.* **1993**, *99*, 4233.

**Table 1.** Ionic van der Waals Parameters Used in the Simulations<sup>a</sup>

force field	potassium		sodium		chloride	
	$r$	$\epsilon$	$r$	$\epsilon$	$r$	$\epsilon$
AMOEBA	3.71	0.35	3.02	0.26	4.13	0.34
OPLS-AA	5.538932	0.000328	3.738298	0.002772	4.958184	0.1180
CHARMM27	3.5275	0.0870	2.7275	0.0469	4.5400	0.1500

<sup>a</sup> Parameters are given as  $r$ , the ionic diameter in angstroms, and  $\epsilon$ , the well-depth in kcal/mol, associated with the minimum of the van der Waals interaction. The CHARMM27 parameters are from Beglov and Roux,<sup>72</sup> while the OPLS-AA parameters are from Åqvist.<sup>19</sup> CHARMM27 and OPLS-AA use a Lennard-Jones function, while AMOEBA uses a buffered 14–7 potential.<sup>76</sup>

CHARMM force field and the slightly modified TIP3P water model supplied by the authentic CHARMM parameter files.<sup>70–72</sup> Parameters for formamide and NMA were drawn from the CHARMM22 model compound parameter set.<sup>66</sup> Because calculations using the AMBER force fields<sup>73,74</sup> also typically use the TIP3P water model and the Åqvist ion parameters, albeit with different amide parameters, the parameter sets simulated here are representative of those used most commonly in biomolecular simulation.

The AMOEBA parameters were drawn from the recently developed AMOEBA force field.<sup>65,75</sup> This force field uses a more complex electrostatic model than most other force fields: each atom has a permanent partial charge, dipole, and quadrupole moment, in contrast to conventional force fields which only include atomic partial charges. Moreover, the force field explicitly represents electronic many-body effects, using a self-consistent dipole polarization procedure.<sup>75</sup> Repulsion–dispersion interactions between pairs of nonbonded atoms are represented by a buffered 14–7 potential.<sup>76</sup> The AMOEBA water model accurately reproduces a wide variety of in vacuo and liquid properties.<sup>65</sup> Parameters for a series of small organic compounds, including hydrocarbons, alcohols, amines, amides, thiols, and aromatics have been developed in a similar fashion and will be presented in a later publication. The parameters for water, formamide, and NMA were held fixed at the previously determined values for the purposes of the present calculations; only the ionic van der Waals parameters were adjusted. Table 1 compares the values used to represent the ions in the different parameter sets. It is immediately apparent there is considerable variation between the three parameter sets. Most notably, OPLS-AA and CHARMM27 both use very small  $\epsilon$  values for the ions.

The AMOEBA dipole polarizabilities of potassium, sodium, and chloride ions were set to 0.78, 0.12, and 4.00 Å<sup>3</sup>, respectively. The values used for the cations are in good agreement with ab initio MP2 correlated results for both K<sup>+</sup><sup>46</sup> and Na<sup>+</sup>,<sup>77</sup> and small enough that polarization of the ions themselves does not play a significant role in the results reported here. For Cl<sup>−</sup> in the gas phase, various workers<sup>78,79</sup> agree on a polarizability value near 5.5 Å<sup>3</sup>, but there is general consensus that this large value is reduced in clusters and condensed phase. Most previous empirical models for the chloride anion<sup>56,59,61</sup> have used polarizabilities in the range 3.25–3.7 Å<sup>3</sup>, in accord with the spectrum of experimental values derived from molar refractivity measurements.<sup>80</sup> Recently, Jungwirth and Tobias<sup>81</sup> have used high-level

quantum calculations on solvated Cl<sup>−</sup> to suggest that a polarizability of 4.0 Å<sup>3</sup> is more appropriate for chloride in water. As discussed below, we have independently found that a chloride polarizability of 4.0 Å<sup>3</sup> is necessary in the AMOEBA formalism to optimally match experimental thermodynamic data for a series of small chloride–water clusters.

**2.2. Cluster Calculations.** Using the AMOEBA force field, we performed stochastic molecular dynamics simulations of clusters of 1–6 water molecules with a single chloride ion, plus a simulation of an isolated water molecule. The equations of motion were integrated using a velocity Verlet implementation of Langevin dynamics. A time step of 0.1 fs was required to produce stable trajectories. The simulations were run for a total of 2 ns for each cluster.

The stepwise hydration enthalpy for chloride was calculated as

$$\Delta H_{\text{hyd}}(n) = \langle E_{n,\text{Cl}} \rangle - \langle E_{n-1,\text{Cl}} \rangle - \langle E_{\text{H}_2\text{O}} \rangle \quad (1)$$

where  $n$  is the number of water molecules,  $\langle E_{n,\text{Cl}} \rangle$  is the average potential energy over the simulation with  $n$  waters and a chloride, and  $\langle E_{\text{H}_2\text{O}} \rangle$  is the average potential energy of an isolated water molecule.

The experimental enthalpies were determined from mass spectroscopic equilibrium data using van't Hoff analysis across a range of temperatures, with the explicit assumption that the binding enthalpy is temperature-independent.<sup>82–84</sup> Accordingly, all cluster simulations were run at 298 K.

**2.3. Molecular Dynamics and Free Energy Simulations.** The absolute solvation free energy for potassium and chloride was calculated using free energy perturbation and molecular dynamics. The calculation was performed in two stages, growth and charging. First, the ion was placed at the origin of a preequilibrated box of solvent containing either 216 water molecules in an 18.643 Å cube or 100 formamide molecules in an 18.778 Å cube. The ion's charge and polarization were set to zero, while its van der Waals parameters were assigned according to

$$\begin{aligned} r(\lambda) &= 1 + \lambda(r_{\text{final}} - 1) \\ \epsilon(\lambda) &= \lambda\epsilon_{\text{final}} \end{aligned} \quad (2)$$

with  $\lambda = (0.01, 0.05, 0.1, 0.2, 0.3, 0.4, 0.5, 0.6, 0.7, 0.8, 0.9, 1.0)$ . For each value of  $\lambda$ , energy minimization was performed until the RMS gradient per atom was less than 1.0 kcal/(mol Å). From that point, 200 ps of constant volume molecular dynamics was performed, with a time step of 1 fs. Coordinates were saved every 0.1 ps. The first 50 ps of each trajectory was discarded as equilibration, while the final 150 ps was analyzed. The system temperature was held at 300 K using the Berendsen weak coupling thermostat with a time constant of 0.1 ps.<sup>85</sup> For simulations containing TIP3P water,<sup>68</sup> the water molecules were held rigid using the RATTLE algorithm.<sup>86</sup> Long-range electrostatics were held rigid using the RATTLE algorithm.<sup>86</sup> Long-range electrostatics for CHARMM27 and OPLS-AA were treated using particle mesh Ewald (PME) summation,<sup>87,88</sup> while conventional Ewald summation<sup>65,89</sup> for polarizable atomic multipole interactions was used for AMOEBA. The Ewald cutoff distance for real space interactions was set to 9 Å, and the Ewald coefficient was 0.42 Å<sup>−1</sup>. In all cases, “tin foil” boundary conditions were applied. The PME calculations used a 30 × 30 × 30 charge grid and eighth-order B-spline interpolation. van der Waals interactions were reduced to zero at 12 Å using a window-based energy switch method. All molecular mechanics calculations were run using TINKER version 3.9.<sup>90</sup> Each trajectory with a nonpolarizable force field

(70) Foloppe, N.; MacKerell, A. D., Jr. *J. Comput. Chem.* **2000**, *21*, 86.  
 (71) Banavali, N.; MacKerell, A. D., Jr. *J. Comput. Chem.* **2000**, *21*, 105.  
 (72) Beglov, D.; Roux, B. *J. Chem. Phys.* **1994**, *100*, 9050.  
 (73) Cornell, W. D.; Cieplak, P.; Bayly, C. I.; Gould, I. R.; Merz, K. M., Jr.; Ferguson, D. M.; Spellmeyer, D. C.; Fox, T.; Caldwell, J. W.; Kollman, P. A. *J. Am. Chem. Soc.* **1995**, *117*, 5179.  
 (74) Wang, J.; Cieplak, P.; Kollman, P. A. *J. Comput. Chem.* **2000**, *21*, 1049.  
 (75) Ren, P.; Ponder, J. W. *J. Comput. Chem.* **2002**, *23*, 1497.  
 (76) Halgren, T. A. *J. Am. Chem. Soc.* **1992**, *114*, 7827.  
 (77) Derepas, A.-L.; Soudan, J.-M.; Brenner, V.; Dognon, J.-P.; Millié, P. *J. Comput. Chem.* **2002**, *23*, 1013.  
 (78) Wong, D. E.; Dunning, T. H. *J. Chem. Phys.* **1994**, *100*, 2975.  
 (79) Hättig, C.; Hess, B. A. *J. Chem. Phys.* **1998**, *108*, 3863.  
 (80) Marcus, Y. *Ion Properties*; Marcel Dekker: New York, 1997.  
 (81) Jungwirth, P.; Tobias, D. J. *J. Phys. Chem. A* **2002**, *106*, 379.  
 (82) Hiraoka, K.; Mizuse, S.; Yamabe, S. *J. Phys. Chem.* **1988**, *92*, 3943.

(83) Džidic, I.; Kebarle, P. *J. Phys. Chem.* **1970**, *74*, 1466.  
 (84) Kebarle, P. *Annu. Rev. Phys. Chem.* **1977**, *28*, 445.  
 (85) Berendsen, H. J. C.; Postma, J. P. M.; van Gunsteren, W. F.; DiNola, A.; Haak, J. R. *J. Chem. Phys.* **1984**, *81*, 3684.  
 (86) Andersen, H. C. *J. Comput. Phys.* **1983**, *52*, 24.  
 (87) Darden, T. A.; York, D. M.; Pedersen, L. G. *J. Chem. Phys.* **1993**, *98*, 10089.  
 (88) Essmann, U.; Perera, L.; Berkowitz, M. L.; Darden, T.; Lee, H.; Pedersen, L. G. *J. Chem. Phys.* **1995**, *103*, 8577.  
 (89) Perram, J. W.; Petersen, H. G.; De Leeuw, S. W. *Mol. Phys.* **1988**, *65*, 875.

required just under 1 day of CPU time on a 950 MHz Athlon running Linux, while each AMOEBA simulation took slightly more than 7 days.

The final structure from the  $\lambda = 1$  particle growth simulation was used as the starting structure for each trajectory in the charging portion. For these calculations, the charge and polarizability were set according to

$$\begin{aligned} q(\lambda) &= \lambda q_{\text{final}} \\ \alpha(\lambda) &= \lambda \alpha_{\text{final}} \end{aligned} \quad (3)$$

with  $\lambda = (0, 0.1, 0.2, 0.3, 0.4, 0.5, 0.6, 0.7, 0.8, 0.9, 1.0)$ . The  $\lambda = 1$  trajectory from the growth stage was also used as the  $\lambda = 0$  trajectory for the charging stage. The molecular dynamics protocol was identical to that used for the particle growth.

The solvation free energy for sodium was calculated starting from the final structure of the potassium charging calculation. The van der Waals parameters were changed linearly from potassium to sodium values, with 200 ps trajectories run at  $\lambda = (0.3, 0.6, 0.9, 1.0)$ . The AMOEBA sodium calculations were executed using a target radius of 3.14 for sodium, and an additional 200 ps simulation was run at  $r = 3.02$  to produce the final free energy. This was necessary because our choice for the radius changed after the free energy simulations were begun.

The Helmholtz solvation free energy was calculated from these trajectories using the free energy perturbation method.<sup>91,92</sup> In this approach, the free energy change upon altering force field parameters is estimated according to

$$\Delta A = -k_{\text{B}}T \ln \langle \exp\{(E - E^*)/k_{\text{B}}T\} \rangle \quad (4)$$

where  $E$  and  $E^*$  are the potential energy of the system using the original and perturbed parameters, respectively.

The standard approach to estimating  $\Delta A(\lambda_i \rightarrow \lambda_{i+1})$  is double-wide sampling,<sup>93</sup> where the forward and reverse perturbations are averaged according to

$$\Delta A = -\frac{k_{\text{B}}T}{2} (\ln \langle \exp\{(E_{\lambda_i} - E_{\lambda_{i+1}})/k_{\text{B}}T\} \rangle_{\lambda_i} - \ln \langle \exp\{(E_{\lambda_{i+1}} - E_{\lambda_i})/k_{\text{B}}T\} \rangle_{\lambda_{i+1}}) \quad (5)$$

In this notation,  $E_{\lambda_i}$  is the system's potential energy calculated with the parameters set to the  $i$ th  $\lambda$  value, and the subscript on the angle bracket indicates which molecular dynamics trajectory was used for averaging. The advantage of this approach is that the difference between the forward and reverse perturbations can be used as a rough estimate of the statistical uncertainty. However, the error in the perturbation formalism grows rapidly with the magnitude of the perturbation, so we instead chose to calculate the free energy in half-steps as

$$\begin{aligned} \Delta A\left(i \rightarrow i + \frac{1}{2}\right) &= -k_{\text{B}}T \ln \langle \exp\{(E_{\lambda_i} - E_{\lambda_{i+1/2}})/k_{\text{B}}T\} \rangle_{\lambda_i} \\ \Delta A\left(i + \frac{1}{2} \rightarrow i + 1\right) &= k_{\text{B}}T \ln \langle \exp\{(E_{\lambda_{i+1/2}} - E_{\lambda_{i+1}})/k_{\text{B}}T\} \rangle_{\lambda_{i+1}} \end{aligned} \quad (6)$$

Because of the difficulties involved in a particle growth simulation with  $\lambda = 0$ ,  $\Delta A(0 \rightarrow 0.01)$  was calculated solely by perturbation from the  $\lambda = 0.01$  simulation. There is no comparable difficulty for particle charging.

In assessing the results of free energy simulations, it is critical to estimate the uncertainty in the results. The most common practice is

to use the difference between forward and backward perturbations. However, the degree of hysteresis does not necessarily correlate with the statistical confidence intervals.

As an alternative, we applied a bootstrap Monte Carlo procedure to estimate the error.<sup>94</sup> Using this technique, we could estimate the uncertainty for a particular perturbation step directly from the data. For a set of  $N$  data points,  $N$  points were chosen at random with duplication allowed, and the free energy difference was computed using eq 4. The statistical uncertainty is estimated as the standard deviation of the free energy difference over many Monte Carlo trials.

When solvation and transfer free energies are computed as the sum of many perturbation steps, the statistical uncertainties for the individual steps do not simply add. If the errors were known to be normally distributed and uncorrelated, the overall standard deviation could be computed as the square root of the sum of the variances computed for the individual perturbation steps. However, it would not be surprising if the errors in the upward and downward half-steps from a given simulation were correlated. To account for this correlation, the bootstrap procedure was applied simultaneously to all of the free energy perturbation steps. For example, a single Monte Carlo trial for computing the solvation free energy of potassium in water would involve selecting  $N$  points and computing  $\Delta A$  for each perturbation half-step in the growth and charging stages, and summing. The standard deviation of that sum over 1000 trials is reported as the uncertainty in the free energy.

Another method for estimating the statistical uncertainty is to compute the standard error while accounting for correlations in the time series. This is done by computing the statistical inefficiency of the time series.<sup>95</sup> For the free energy  $A$ , the relevant time series is  $\Omega(t) = \exp\{(E(t) - E^*(t))/k_{\text{B}}T\}$ . The variance in the free energy then becomes

$$\sigma^2(A) = k_{\text{B}}T \frac{\sigma^2(\Omega(t))}{\langle \Omega(t) \rangle} \quad (7)$$

where  $\sigma^2$  denotes the variance. The overall statistical uncertainty can then be calculated as the standard error, once correlations in the time series are properly accounted for. The resulting uncertainty can be written as

$$u(A) = \sigma(A) \sqrt{\frac{s}{N}} \quad (8)$$

where  $N$  is the number of points in the time series, and  $s$  is the statistical inefficiency of  $\Omega$  calculated using block averaging, as described by Allen and Tildesley.<sup>95</sup> The plateau value for  $s$  was taken to be the average of the value calculated dividing the trajectory into 5–15 blocks, after manual examination of a number of trajectories. The uncertainty for the free energy of solvation for an ion was computed by summing the variances for each step and taking the square root. Although uncertainties computed in this manner are systematically larger than those computed by the bootstrap method, the difference is quite small, typically less than 0.05 kcal/mol for single ion solvation free energies. For this reason, only the bootstrap Monte Carlo uncertainties are reported.

In recent years, several authors have considered the issue of system size dependence and periodicity artifacts in calculations of ionic hydration.<sup>96–100</sup> This work would seem to indicate that such artifacts would be small in our simulations, given the relatively large system size and the high dielectric of the solvents. In particular, the work of Bogusz et al. demonstrates that the ionic solvation free energy is not sensitive to these corrections for systems of the size considered here,

(90) Ponder, J. W. TINKER: Software Tools for Molecular Design, Version 3.9; Saint Louis, MO, 2001.

(91) Torrie, G. M.; Valleau, J. P. *Chem. Phys. Lett.* **1974**, *28*, 578.

(92) Postma, J. P. M.; Berendsen, H. J. C.; Haak, J. R. *Faraday Symp. Chem. Soc.* **1982**, *17*, 55.

(93) Jorgensen, W. L.; Ravimohan, C. J. *Chem. Phys.* **1985**, *83*, 3050.

(94) Press, W. H.; Teukolsky, S. A.; Vetterling, W. T.; Flannery, B. P. *Numerical Recipes in Fortran*, 2nd ed.; Cambridge University Press: Cambridge, 1992.

(95) Allen, M. P.; Tildesley, D. J. *Computer Simulation of Liquids*; Oxford University Press: Oxford, 1987.

**Table 2.** Ion–Water Dimers from Different Force Fields<sup>a</sup>

method	potassium		sodium		chloride	
	energy	distance	energy	distance	energy	distance
AMOEBA	-17.3	2.597	-23.2	2.233	-15.5	3.152
OPLS-AA	-18.2	2.639	-23.9	2.313	-13.6	3.186
CHARMM27	-18.9	2.624	-25.5	2.222	-14.7	3.098
ab initio <sup>b</sup>	-17.8	2.605	-23.6	2.230	-15.4 (-14.5)	3.103

<sup>a</sup> The distances are from the ion to the water oxygen, in angstroms. The energies are the interaction between the ion and water, in kcal/mol. The TIP3P water used for the OPLS-AA and CHARMM27 calculations was held rigid during the minimizations. <sup>b</sup> The ab initio values for the cations are MP2 results with correlation consistent basis sets as reported by Feller et al.<sup>46</sup> The chloride ab initio results are from Xantheas<sup>47</sup> and are at the MP4/aug-cc-pVTZ level with the BSSE corrected energy in parentheses.

when standard Ewald summation is used.<sup>99</sup> Moreover, the pressure artifacts due to a net charged system are irrelevant in the context of a constant volume simulation, because the forces between atoms are unaffected. Given the empirical nature of the suggested correction terms, we believe that the uncertainty introduced by their inclusion is of the same magnitude as the expected error. As a result, no such correction was applied to the present results.

In experimental work transferring ions from the gas to liquid phase, the standard states are typically chosen to be a gas at 1 atm and a 1 molar solution. By contrast, the computer simulations effectively choose the gas-phase standard state to be 1 M. Consequently, the free energy to expand an ideal gas

$$T\Delta S = -k_B T \ln \frac{V_{1\text{atm}}}{V_{1\text{M}}} = -k_B T \ln(24.46) = -3.197 k_B T \quad (9)$$

must be included. As a result, 1.9 kcal/mol was added to each of the simulated single ion solvation free energies and 3.8 kcal/mol was added to the salt free energies. The experimental data from Schmid et al.<sup>38</sup> use a 1 M gas as the reference state, so the same correction was applied to their results as well.

### 3. Results

**3.1. Ion–Solvent Dimers.** Although liquid-phase properties are of primary chemical and biophysical interest, the comparative simplicity of gas-phase behavior allows us to examine ion–solvent behavior without concerns about statistical sampling. Moreover, high-level quantum calculations are at present only possible for the gas phase, unless an implicit solvent model is used.

The AMOEBA cation van der Waals parameters were chosen to match the ab initio calculations on ion–water dimers from Feller et al.<sup>46</sup> For potassium–water, the widely cited experimental value of  $\Delta H_{298} = -17.9$  kcal/mol for the potassium–water interaction<sup>83</sup> is nearly identical to the calculated interaction energy<sup>46</sup> of  $-17.8$  kcal/mol. To reduce the degeneracy in determining  $r$  and  $\epsilon$ , we fit the entire energy–separation curve, rather than just the energy minimum. We then computed the interaction energy and cation–oxygen separation for the minimum energy structure. The results are shown in Table 2. The AMOEBA energy is quite similar to the ab initio result, and the distance differs by less than 0.01 Å. For comparison purposes, the calculation was repeated using rigid TIP3P water

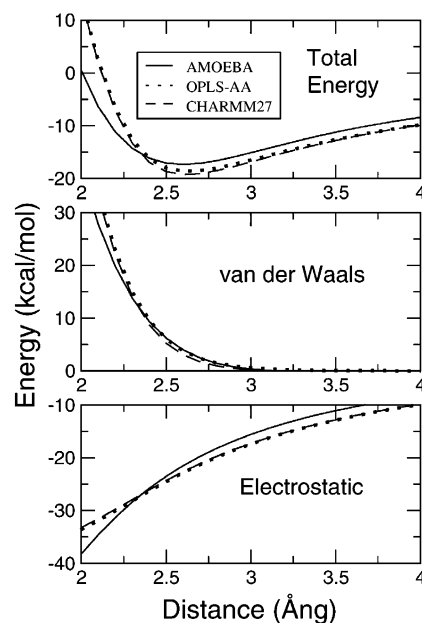


**Figure 1.** Interaction energy between a water molecule and a potassium ion, as a function of the ion–oxygen distance. The top panel shows the total energy, while the middle and bottom panels show the van der Waals and electrostatic components of the energy, respectively.

and the CHARMM27 and OPLS-AA ion parameters. The OPLS-AA and CHARMM27 potassium parameters give too long of a distance, while simultaneously overestimating the favorable interaction. This difficulty is due to the TIP3P water model, which by implicitly including the polarization appropriate to liquid phase water overestimates the gas-phase dipole. As such, it is unlikely that better gas-phase results could be obtained by simply modifying the ionic van der Waals parameters without also altering the water model to the detriment of its liquid behavior. In some sense, this is an unfair comparison, because the TIP3P water model is not intended for use in the gas phase, while the AMOEBA results were fit directly to the quantum data.

Figure 1 shows the potassium–water interaction energy as a function of the ion–oxygen distance for all three parameter sets. As shown by the top panel, the AMOEBA interaction energy is qualitatively different from the nonpolarizable force fields; the interaction energy varies more slowly with distance, with less favorable energies at long distances, but also rising less steeply at short range. A small part of this effect is due to the use in AMOEBA of a buffered 14–7 potential<sup>76</sup> in place of the more common Lennard-Jones van der Waals function. This can be seen in the middle panel. Despite radically different  $r$  and  $\epsilon$  parameters (see Table 1), the OPLS-AA and CHARMM27 ions have very similar van der Waals energy curves.

However, most of the difference between AMOEBA and the other force fields is due to the electrostatic terms. The AMOEBA electrostatic energy drops rapidly as the ion approaches the water, because the ion’s electric field polarizes the water, creating nonadditive favorable interactions. However, at ion–oxygen separations greater than 2.3 Å, the electrostatic attraction is less than for TIP3P water. This effect cannot be captured by a nonpolarizable force field.

For the sodium–water dimer, the OPLS-AA parameters place the minimum at too long a distance, while slightly underestimating the favorability. CHARMM27 has too low an energy at too

(96) Hummer, G.; Pratt, L. R.; Garcia, A. E. *J. Phys. Chem.* **1996**, *100*, 1206.

(97) Hummer, G.; Pratt, L. R.; Garcia, A. E. *J. Chem. Phys.* **1997**, *107*, 9275.

(98) Figueirido, F.; Del Buono, G. S.; Levy, R. M. *J. Chem. Phys.* **1995**, *103*, 6133.

(99) Bogusz, S.; Cheatham, T. E., III; Brooks, B. R. *J. Chem. Phys.* **1998**, *108*, 7070.

(100) Hunenberger, P. H.; McCammon, J. A. *Biophys. Chem.* **1999**, *78*, 69.

**Table 3.** Cation–Amide Dimers from Different Force Fields<sup>a</sup>

solvent	method	potassium		sodium	
		energy	distance	energy	distance
formamide	AMOEBA	−25.67	2.498	−33.44	2.129
	OPLS-AA	−21.31	2.600	−26.26	2.292
	CHARMM27	−23.73	2.541	−30.58	2.156
	ab initio <sup>b</sup>	−26.10		−33.68	
NMA	AMOEBA	−27.74	2.464	−36.36	2.100
	OPLS-AA	−22.04	2.592	−27.14	2.286
	CHARMM27	−24.20	2.537	−31.10	2.152
	ab initio <sup>b</sup>	−30.02		−38.38	

<sup>a</sup> The distances are between the ion and the carbonyl oxygen, in angstroms. The energies are interactions between the ion and amide, with the energy of a minimized isolated amide removed, in kcal/mol. <sup>b</sup> Ab initio results are taken from Siu et al.<sup>106</sup> and are based on calculations using the Gaussian-2 and Gaussian-3 protocols.

short a Na<sup>+</sup>–O distance. These differences from the ab initio results probably could be diminished by modifying the van der Waals parameters of the ion, although as with potassium it seems that the distance and energy cannot be matched simultaneously while using the TIP3P water model. Several experimental values are available for the sodium–water binding enthalpy<sup>101</sup> including  $\Delta H_{298} = -24.0$  kcal/mol from mass spectrometric measurements by Džidić and Kabarle,<sup>83</sup> and a collision-induced dissociation (CID) value of  $\Delta H_0 = -22.6 \pm 1.8$  kcal/mol from Dalleska et al.<sup>102</sup> Both the OPLS-AA and the AMOEBA values lie within this experimental range.

For the chloride ion, we used quantum calculations of Xantheas on the chloride–water dimer as the basis for parametrization.<sup>47</sup> Other quantum results available for this system are quantitatively similar.<sup>103,104</sup> As compared with the cation systems, molecular orbital calculations are more problematic for chloride–water due to the large basis set superposition error (BSSE). A recent analysis based on a series of computations extrapolated to the complete basis set (CBS) limit suggests that interaction energies without BSSE correction are more reliable than corrected energies for moderate basis sets.<sup>105</sup> In addition, the quantum results yield interaction energies somewhat inconsistent with the experimental enthalpy of the chloride–water dimer.<sup>82</sup> As shown in Table 2, the CHARMM27 parameters match ab initio results from Xantheas fairly well, although the interaction energy is smaller in magnitude than the uncorrected value of Xantheas. OPLS-AA underestimates the dimer binding with too long of a Cl<sup>−</sup>–O distance, while AMOEBA gives a reasonable interaction energy with somewhat too long of a distance. Interestingly, the polarizability of the ion is anticorrelated with the dimer binding energy. Given the difficulties involved in performing high-level quantum calculations on anions, we chose to also parametrize the AMOEBA chloride ion against experimental data as discussed in section 3.2.

We also computed the minimum energy structures for the cations interacting with formamide and NMA, as given in Table 3. The AMOEBA force field shows much smaller cation–oxygen separations than the other force fields, with concomitantly more favorable interaction energies. OPLS-AA has

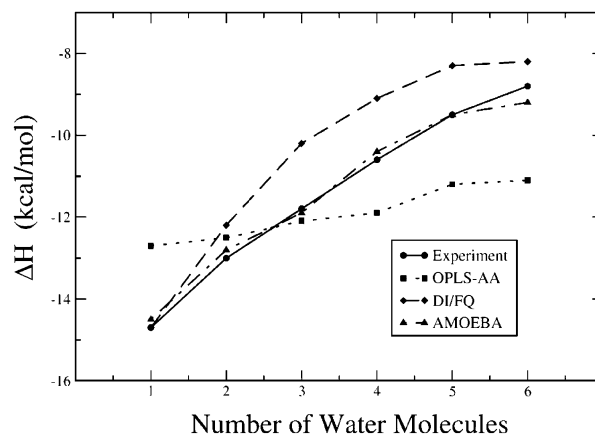


**Figure 2.** Differential stepwise enthalpy of hydration for chloride ion. The experimental values are from Hiraoka et al.<sup>82</sup> The OPLS-AA and DI/FQ values are taken from the paper by Stuart and Berne.<sup>56</sup> The OPLS-AA results were calculated using the TIP4P water model, while DI/FQ indicates the polarizable fluctuating charge water model, with chloride polarization represented using a Drude oscillator model.<sup>56</sup> The AMOEBA differential enthalpy values for  $n = 1$ –6 water molecules are  $-14.5$ ,  $-12.9$ ,  $-11.9$ ,  $-10.4$ ,  $-9.5$ , and  $-9.2$  kcal/mol, respectively.

consistently longer distances and less favorable energies than CHARMM27. Recent ab initio results<sup>106</sup> from a protocol designed to reproduce thermochemical data yield interaction energies that are uniformly slightly larger than AMOEBA and dramatically larger than the nonpolarizable force fields. Klassen et al.<sup>107</sup> have used CID threshold data to experimentally determine the binding enthalpy of Na<sup>+</sup> and K<sup>+</sup> to NMA. Their  $\Delta H_{298}^0$  values of  $-30.4$  and  $-35.7$  kcal/mol for K<sup>+</sup>–NMA and Na<sup>+</sup>–NMA, respectively, are also in reasonable agreement with the AMOEBA-derived values.

**3.2. Chloride–Water Clusters.** Because of the difficulties involved in ab initio computation of the energies of anion–water clusters,<sup>47,104</sup> we compared our van der Waals parameters for chloride with experimental data, specifically the enthalpy of formation of a chloride–water dimer. The stepwise hydration enthalpy for chloride water clusters up to  $n = 6$  was then computed as described above.

Figure 2 presents the simulated and experimental hydration enthalpies.<sup>82</sup> For all clusters, the AMOEBA model shows excellent agreement; the differences between the calculated and experimental values are comparable to the experimental uncertainties (0.3–0.4 kcal/mol). The agreement is least satisfactory for the  $n = 6$  case, where the presence of multiple configurations slows the statistical convergence of the simulation.

For comparison, Figure 2 also shows previously published work using the nonpolarizable TIP4P and polarizable FQ water models.<sup>56</sup> The TIP4P results underestimate the favorability of dimer formation, but then overestimate the favorability of adding water molecules. The FQ water model, which explicitly includes electronic polarization using the fluctuating charge formalism, matches the dimer enthalpy very well, but underestimates the favorability of subsequent cluster growth. Thus, the explicit inclusion of polarization is not the sole reason for the success of the AMOEBA model.

In addition, AMOEBA calculations for the chloride–water clusters were performed using two smaller values of the chloride

(101) Hyoyau, S.; Norrman, K.; McMahon, T. B.; Ohanessian, G. *J. Am. Chem. Soc.* **1999**, *121*, 8864.

(102) Dalleska, N. F.; Tjelja, B. L.; Armentrout, P. B. *J. Phys. Chem.* **1994**, *98*, 4191.

(103) Gora, R. W.; Roszak, S.; Leszczynski, J. *Chem. Phys. Lett.* **2000**, *325*, 7.

(104) Masamura, M. *J. Phys. Chem. A* **2002**, *106*, 8925.

(105) Masamura, M. *Theor. Chem. Acc.* **2001**, *106*, 301.

(106) Siu, F. W.; Ma, N. L.; Tsang, C. W. *J. Chem. Phys.* **2001**, *114*, 7045.

(107) Klassen, J. S.; Anderson, S. G.; Blades, A. T.; Kebarle, P. *J. Phys. Chem.* **1996**, *100*, 14218.

**Table 4.**  $\Delta A_{\text{solv}}$  for Ions in Water and Formamide<sup>a</sup>

solvent	method	potassium	sodium	K <sup>+</sup> → Na <sup>+</sup>	chloride
water	AMOEBA	-72.6 ± 0.1	-89.9 ± 0.1	-17.3 ± 0.0	-84.6 ± 0.1
	OPLS-AA	-65.7 ± 0.1	-83.9 ± 0.1	-18.2 ± 0.1	-85.3 ± 0.1
	CHARMM27	-70.3 ± 0.1	-91.0 ± 0.1	-20.7 ± 0.1	-91.2 ± 0.1
	Schmid <sup>38</sup>	-69.3	-86.8	-17.5	-87.2
	Friedman <sup>24</sup>	-80.8	-98.3	-17.5	-75.8
	Tissandier <sup>42</sup>	-84.1	-101.3	-17.2	-72.7
forma- mide	AMOEBA	-81.3 ± 0.1	-99.8 ± 0.1	-18.6 ± 0.0	-72.1 ± 0.3
	OPLS-AA	-66.3 ± 0.1	-83.2 ± 0.1	-16.9 ± 0.1	-59.6 ± 0.3
	CHARMM27	-76.1 ± 0.1	-95.9 ± 0.1	-19.8 ± 0.1	-79.1 ± 0.1
	Cox+Schmid			-18.2	

<sup>a</sup> Sodium was calculated by transforming potassium to sodium, starting from the final structure of the potassium charging simulation. The error bars on the simulated free energies are statistical uncertainties. The Cox+Schmid free energy difference between K<sup>+</sup> and Na<sup>+</sup> in formamide is estimated from the Cox et al.<sup>25</sup> experimental transfer energy of KCl and NaCl from water to formamide combined with the Schmid et al. water result.<sup>38</sup> All free energies are in kcal/mol. Extracting individual ion solvation free energies from experiments requires an extrathermodynamic assumption, which cancels upon comparing the solvation of two cations.

polarizability (3.25 and 3.7 Å<sup>3</sup> vs 4.0 Å<sup>3</sup>). Both of these alternative polarizability values yield hydration enthalpies that are not as negative as was obtained with our suggested value of 4.0 Å<sup>3</sup>. The differences are small for the clusters containing three or fewer waters, but are larger for some of the bigger clusters. For example, the incremental  $\Delta H$  for adding a fourth water to form the Cl<sup>-</sup>(H<sub>2</sub>O)<sub>4</sub> cluster is 0.5–1.0 kcal/mol less negative than the experimental value when using the smaller chloride polarizabilities.

**3.3. Ion Solvation.** Table 4 summarizes the results of the solvation free energy calculations for the ions in water and formamide. For water, the results are compared to three sets of model values based on experimental data due to Schmid et al.,<sup>38</sup> Friedman and Krishnan,<sup>24</sup> and Tissandier et al.<sup>42</sup> The single ion values from the three models differ by as much as 15 kcal/mol. In contrast, the three sets give consistent numbers for the difference between the solvation free energy of potassium and sodium. This occurs because the single ion values are not directly accessible experimentally. Rather, dividing the solvation of whole salts into contributions from anions and cations requires additional assumptions which cannot be tested experimentally. The model of Schmid et al. derives the anion and cation thermodynamic components based on a self-consistent thermodynamic analysis, while Friedman and Krishnan make the TATB assumption, and Tissandier et al. use a cluster-pair assumption.

In water, CHARMM27 and AMOEBA have cation solvation free energies that lie in the middle of the model values, while the OPLS-AA value is not low enough. For chloride, CHARMM27 has too low of a solvation free energy as compared to the three experiment-derived models, while the OPLS-AA and AMOEBA values are within the model range.

For the relative solvation free energy of potassium and sodium, all three models agree due to the cancelation of extrathermodynamic assumptions. The AMOEBA force field exhibits the best agreement for these relative free energies. OPLS-AA overestimates the difference in water and underestimates it in formamide, while CHARMM27 significantly overestimates the relative energy in both solvents.

**3.4. Solvation Free Energies for Whole Salts.** In contrast to individual ions, the solvation and transfer thermodynamics of whole salts and electrolytes are true experimental values that are free of extrathermodynamic assumptions. Not surprisingly,

**Table 5.**  $\Delta A_{\text{solv}}$  for Whole Salts<sup>a</sup>

solvent	method	KCl	NaCl
water	AMOEBA	-157.2 ± 0.1	-174.4 ± 0.1
	OPLS-AA	-151.0 ± 0.1	-169.2 ± 0.1
	CHARMM27	-161.5 ± 0.1	-182.2 ± 0.1
	Schmid <sup>38</sup>	-156.5	-174.0
	Friedman <sup>24</sup>	-156.6	-174.1
	Tissandier <sup>42</sup>	-156.8	-174.0
formamide	AMOEBA	-153.4 ± 0.3	-172.0 ± 0.3
	OPLS-AA	-125.9 ± 0.4	-142.8 ± 0.4
	CHARMM27	-155.3 ± 0.1	-175.1 ± 0.1
	Cox+Schmid <sup>b</sup>	-154.4	-172.6

<sup>a</sup> The experimental numbers for water were derived by summing the anion and cation free energies from Table 4. Note that summing anion and cation solvation free energies causes the extrathermodynamic assumption to cancel. <sup>b</sup> The Cox+Schmid solvation free energies for formamide were computed by combining the water solvation data from Schmid et al.<sup>38</sup> with the transfer free energies from Cox et al.<sup>25</sup> All free energies are in kcal/mol.

the three models, which are based on whole salt solvation values, differ by only 0.3 kcal/mol for KCl and 0.1 kcal/mol for NaCl, while the derived single ion values differ by roughly 15 kcal/mol. By combining the results from the individual potassium, sodium, and chloride simulations, we can compute salt solvation free energies to compare with experiment. Table 5 shows the results for solvation of KCl and NaCl in water and formamide. Absolute solvation free energies of KCl and NaCl in formamide were unavailable, so the experimental free energies of transfer from water to formamide given by Cox et al.<sup>25</sup> were combined with the absolute aqueous solvation values of Schmid et al.<sup>38</sup> The AMOEBA calculations match the experimental results for both salts in both solvents, differing on average by 0.55 kcal/mol, which is less than the presumed uncertainty in the experimental numbers. CHARMM27 and OPLS-AA do not perform nearly as well, with average deviations of 6.7 and 9.8 kcal/mol, respectively.

All three force fields appear to vary systematically from experiment, but in different ways. The OPLS-AA force field underestimates the solvation free energy in all cases, although the numbers for water are significantly closer to experiment. The OPLS-AA solvation free energy is not nearly favorable enough for both salts in formamide. This is as expected, given the small ion–formamide interaction energies from Table 3.

The CHARMM27 parameters, by contrast, overestimate the solvation free energies for the salts and are closer to experiment for formamide than for water. However, examination of the individual ion solvation values suggests significant cancellation of error in formamide. The chloride solvation free energy in water is significantly more negative than any literature value. The free energy in formamide is also much lower than that for AMOEBA, which seems to indicate a problem with the chloride parameters. By contrast, the free energy of solvation of the cations in formamide is not low enough, as compared to AMOEBA. This result could be predicted from the gas-phase calculations, which showed insufficient ion–amide binding energies for the CHARMM27 potential. As a result, the differences cancel and the salt solvation free energies are close to experiment in formamide.

The AMOEBA force field agrees well with experiment for the whole salts, but there is some systematic deviation. The solvation of both salts is slightly overestimated in water and underestimated in formamide. This agreement might be im-



**Table 6.**  $\Delta A_{\text{trans}}$  from Water into Formamide for Whole Salts<sup>a</sup>

method	KCl	NaCl
AMOEBA	$3.8 \pm 0.3$	$2.7 \pm 0.3$
OPLS-AA	$25.1 \pm 0.4$	$26.3 \pm 0.4$
CHARMM27	$6.2 \pm 0.1$	$7.1 \pm 0.2$
experiment	2.2	1.4

<sup>a</sup> The experimental transfer energies are from Table 1 of Cox et al.<sup>25</sup> No extrathermodynamic assumption was required. All free energies are in kcal/mol.

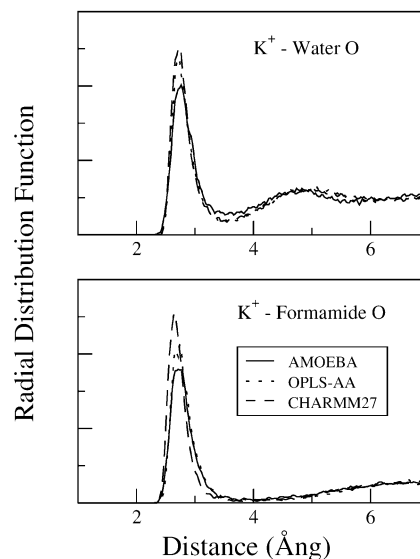
proved by adjusting the ionic vdW parameters, at the cost of diminishing agreement with the gas-phase quantum and experimental results. However, given the uncertainties in all of the possible sources of information, we prefer to balance experiment and quantum calculations in choosing our parameters.

The simulations can also be used to compute the free energy required to transfer electrolytes from water to formamide by taking the difference between the salt solvation free energies shown in Table 5. As with salt solvation, electrolyte transfer free energies can be obtained without recourse to any extra-thermodynamic assumption. The transfer results are shown in Table 6. All three force fields overestimate the stability of salts in water relative to formamide. The CHARMM27 results differ by 4.7 kcal/mol on average, while the OPLS-AA simulations are in error by more than 25 kcal/mol. The simulations with the AMOEBA force field do significantly better, with an average difference of 1.5 kcal/mol. The two nonpolarizable force fields demonstrate significant cancellation of error in this calculation, in that CHARMM27 overestimates the solvation in both solvents and OPLS-AA underestimates it, with the result that the error in transfer energy is smaller than the error in the underlying salt solvation free energy.

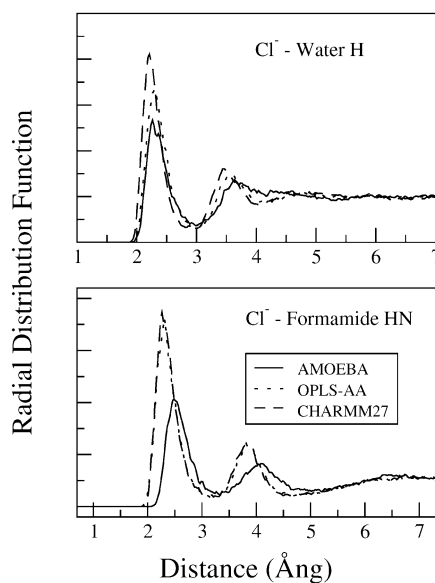
**3.5. Solvent Structure around Ions.** The computed solvation free energies describe the relative stability of ions as a function of solvent and force field, without revealing much about the structure of the solvent around the ion. However, generating the correct ensemble of structures is just as important as obtaining the correct stability value. This is especially true once we move the ions from neat liquids to more complex systems, such as ion channels, where a much narrower range of conformations may be available. Accordingly, we computed radial distribution functions for solvent atoms about the ions.

Figure 3 shows the distribution of solvent oxygen atoms about the potassium ion. The results for the nonpolarizable force fields differ strikingly from the AMOEBA results. First, the contact peak is significantly higher. In water, the corresponding minimum is also deeper. Figure 4 shows the radial distribution for polar hydrogens (both water hydrogens, and the amide hydrogens from formamide) about the chloride ion. As in Figure 3, the first peak is dramatically higher for the nonpolarizable force fields, as compared to AMOEBA. Moreover, the second peak is more pronounced and shifted to shorter distances.

Taken together, the two figures clearly indicate the nonpolarizable force fields significantly overstructure the solvent. This makes intuitive sense; with fixed partial charges and rigid molecular geometry, favorable electrostatic interactions are only possible for a relatively restricted range of geometries. By comparison, the explicit polarizability of the AMOEBA force field allows the solvent molecules to interact favorably in a wider variety of conformations. Similar behavior was seen in the work of Stuart and Berne, who observed that TIP4P water



**Figure 3.** Radial distribution functions for solvent about potassium ion. The upper plot shows the distribution of water oxygens, while the lower plot shows the distribution of formamide oxygens. The data are taken from the last window of the free energy simulations, where the ion takes its final parameters.



**Figure 4.** Radial distribution functions for solvent about chloride ion. The upper plot shows the distribution of water hydrogens, while the lower plot shows the distribution of formamide amide hydrogens. The data are taken from the last window of the free energy simulations, where the ion takes its final parameters.

had a much larger first peak about chloride as compared to the polarizable DI/FQ model.<sup>56</sup>

The most dramatic feature of Figure 4 is the difference in the location of the first peak of formamide amide–hydrogen distribution. The AMOEBA peak is 2.5 Å from the chloride, while the CHARMM27 and OPLS-AA distributions peak at 2.3 Å. The location of the first minimum and second peak are also shifted accordingly. The CHARMM27 and OPLS-AA radial distribution functions are nearly identical. This seems remarkable, given that the two force fields use different formamide parameters (as opposed to the calculations in water, where both use the TIP3P model). As such, it may indicate a systematic problem due to the neglect of polarization.

**Table 7.** Coordination Number for Ions in Bulk Solvent<sup>a</sup>

solvent	force field	potassium	sodium	chloride
water	AMOEBA	7.0	6.0	6.0
	OPLS-AA	6.6	6.5	7.0
	CHARMM27	6.9	5.9	7.2
formamide	AMOEBA	6.3	6.0	5.9
	OPLS-AA	6.9	6.0	7.1
	CHARMM27	6.6	5.9	7.5

<sup>a</sup> Values reported are calculated by integrating over the water–ion radial distribution functions (shown for K<sup>+</sup> and Cl<sup>−</sup> in Figures 3 and 4, respectively). The position of the first minimum in the radial distribution function was taken as the outer limit of the first solvation shell.

In Table 7, we report the computed coordination numbers for the ions using

$$N_c = \frac{4\pi N_{\text{pair}}}{V} \sum_{r_{\text{min}}}^{r_{\text{min}}} g(r) r^2 \Delta r \quad (10)$$

where  $N_{\text{pair}}$  is the number of pairs in the distribution function,  $V$  is the system volume,  $g(r)$  is the radial distribution function, and  $r_{\text{min}}$  is the location of the first minimum of  $g(r)$ .  $\Delta r$  is the bin width used to compute  $g(r)$ , set to 0.025 Å. Because of uncertainty in the location of the minimum, the uncertainty in  $N_c$  is roughly 0.3.

For the cations, the results for the different force fields are qualitatively similar, indicating that the basic mechanism of solvation is similar. However, the coordination of chloride is significantly larger for the nonpolarizable force fields as compared to AMOEBA. Similar behavior was seen in the chloride–water cluster simulations of Stuart and Berne.<sup>56</sup> It is interesting that coordination number dependence on explicit polarizability is maintained across solvents for the anion, while being absent for the cation. In principle, the coordination number for ions in water can be measured experimentally using a variety of techniques including X-ray and neutron diffraction, EXAFS, and NMR.<sup>108</sup> X-ray and neutron estimates based on analysis of experimentally derived  $g(r)$  curves provide the most direct comparison with coordination numbers from simulation. However, there is widespread disagreement in the literature, with reported hydration numbers varying from 4 to 8 water molecules for both the sodium and the potassium ion.<sup>80,108–110</sup> Experimental coordination number estimates for chloride ion are consistently near 6 with a typical range of 5.3–6.2 water molecules.<sup>111</sup>

## 4. Discussion

**4.1. Interpretation of Solvation Free Energies.** When Tables 4–6 were examined, it is apparent that the AMOEBA force field simulations agree very well with all available experimental quantities, other than the single ion solvation free energies. All of the experimental quantities derived without reference to the TATB or other external assumptions – the difference between the sodium and potassium single ion solvation free energies, the solvation free energies for salts, and the transfer free energies for salts – are accurately reproduced.

In this context, we can reconsider the single ion solvation results, shown in Table 4. One possible interpretation is that

the AMOEBA results reflect compensating errors in the solvation free energy for both cations and for chloride, in such a way that the errors precisely cancel for both whole salts in two different solvents. This would be remarkable, considering that the ion parameters were chosen to match microscopic results in water (high-level ab initio results for the ion–water dimers and experimental enthalpies for chloride–water clusters) and were not adjusted for the free energy calculations. Alternatively, we can argue that the separations of the experimental values into cation and anion components seen in the literature are flawed. This seems reasonable, given the controversy in the experimental literature,<sup>20,22,24–27,38,42</sup> and the essential unverifiability of the various assumptions involved. Indeed, commonly cited reviews of ion solvation thermodynamics directly state that the single ion values are suspect because of problems with the manner in which they were derived.<sup>20,24</sup> By comparison, the cation and anion simulations are completely independent, and the parameters and methods are subject to independent verification against a variety of experimental and theoretical results. As a consequence, we believe that the present results should be considered the most reliable reference values for single ion solvation.

**4.2. Explicit Polarization and Transferability of Parameters.** The present work demonstrates that the AMOEBA force field is capable of reproducing a number of experimental and theoretical results for ions, both in vacuo and in the liquid phase, using a single set of parameters. The AMOEBA parameters are transferable in large part because the force field explicitly includes nonadditive polarization. This is in contrast to more conventional force fields such as CHARMM27 and OPLS-AA which fix the atomic partial charges. This means that assumptions must be made during the parametrization process about the environment in which the parameters will be used, and the resulting parameters will not always function well if those assumptions are violated. For example, TIP3P water has a dipole moment of 2.35 D,<sup>68</sup> which is not far from the liquid-phase value of 2.6–3.0 D, but is significantly higher than the gas-phase value of 1.86 D.<sup>112</sup> This is not a problem if the model is used to describe bulk water, but as shown in Table 2, there are difficulties in modeling gas-phase complexes. CHARMM27 and OPLS-AA both overestimate the potassium–water energy, despite having too long of a separation. CHARMM27 overestimates the sodium–water interaction by an even larger amount, while OPLS-AA yields a better energy value at the cost of a very long Na<sup>+</sup>–O distance. Because both pairwise force fields significantly overestimate the long-range favorability of cation–water interaction (see Figure 1), very large effective ionic radii are necessary to produce reasonable solvation energies.

As a result, the CHARMM27 and OPLS-AA ion parameters perform poorly for the ion–amide dimers. One would expect a nonpolarizable force field which yields correct solvation energies to overestimate the cation–formamide dimer energy, because the amide bulk polarization would be present in the gas-phase calculation. Instead, we see that both force fields severely underestimate the attraction between the cations and the amides, with ion–oxygen distances that appear too large at the minimum energy structures.

The above results make it clear that nonpolarizable ion parameters appropriate for use in liquid water may not be well-

(108) Ohtaki, H. a. R., *T. Monatsh. Chem.* **2001**, *132*, 1237.

(109) Ohtaki, H. a. R., *T. Chem. Rev.* **1993**, *93*, 1157.

(110) Marcus, Y. *Ion Solvation*; John Wiley and Sons: Chichester, 1985.

(111) Cummings, S.; Enderby, J. E.; Neilson, G. W.; Newsome, J. R.; Howe, R. A.; Howells, W. S.; Soper, A. K. *Nature* **1980**, *287*, 714.

(112) Lovas, F. J. *J. Phys. Chem. Ref. Data* **1978**, *7*, 1445.

**Table 8.** Comparison of Proton Solvation Free Energies<sup>a,b</sup>

source (ref)	Schmid <sup>c</sup> (38)	Tissandier (42)	Friedman (24)	Latimer (10)	Marcus (114)	Zhan (53)	Asthağiri <sup>c</sup> (45)	AMOEBA <sup>c</sup> (this work)
H <sup>+</sup>	-249.5	-264.0	-260.5	-253.4*	-251.0	-262.4	-252.7	-252.5*
OH <sup>-</sup>	-117.4	-103.0	-90.6 <sup>d</sup> -106.1**	-114.5**	-102.8	-104.5	-103.4	-116.8**
H <sup>+</sup> + OH <sup>-</sup>	-366.9	-367.0	-351.1 -366.6**	-367.9***	-353.8	-366.9	-356.1	-367.4***

<sup>a</sup> The first five columns contain data which relies on manipulation of previously determined experimental values, while the last three columns are predictions from computer simulations. All values are free energies are in kcal/mol. <sup>b</sup> Some values were not directly available from the reference cited, but were constructed using K<sup>+</sup> or Cl<sup>-</sup> values from the reference and conversion to H<sup>+</sup> or OH<sup>-</sup> values using the conventional values of Fawcett.<sup>113</sup> One asterisk indicates that the K<sup>+</sup> free energy was used after correction by the value  $\Delta A(K^+ \rightarrow H^+) = -179.9$  kcal/mol. Two asterisks indicates the Cl<sup>-</sup> solvation free energy was used following correction by  $\Delta A(Cl^- \rightarrow OH^-) = -30.3$  kcal/mol. <sup>c</sup> The standard state correction provided in eq 9 was applied to the results from Schmid et al., Asthağiri et al., and the present work. <sup>d</sup> The OH<sup>-</sup> value from Friedman and Krishnan appears to be an outlier, so an alternative derived from their Cl<sup>-</sup> value is presented as well.

suited for other venues, such as liquid formamide. This implies that reparametrization may be required for each new environment simulated, an enormous, often impossible, undertaking. Moreover, most biological simulations contain environments with contrasting physical properties. For example, the interior of a membrane is clearly different from the surrounding bulk water or the membrane–water interface. Similarly, the interior of a protein is quite different from the surface, which in turn differs from bulk solution. For simple ions, one can handle these issues by using multiple sets of van der Waals parameters in place of combination rules, leaving the rest of the force field unchanged. This technique was used by Roux and co-workers<sup>48,49</sup> in simulating potassium permeation in the KcsA channel. Aside from the possible need to reparametrize for every new environment considered, this solution masks a more general problem. When parametrizing proteins, one must fix not only van der Waals parameters but also the atomic partial charges of the side chains and peptide backbone. By analogy with the ionic radii, the parameters appropriate for small peptides in a vacuum or water may not accurately model the interior of a large protein. Because portions of a molecule may sample multiple environments during a simulation (for example, during folding or unfolding of a protein), there is no simple procedure for constructing consistent parameters.

Polarizable force fields can avoid this difficulty by directly representing the molecular response to changes in the environment. The present results demonstrate that parameters derived for the gas phase can be used successfully in multiple solvents, provided polarization is correctly accounted for. This allows the AMOEBA calculations to make direct predictions about ionic solvation. By contrast, the nonpolarizable force fields must use the experimental numbers as input and thus cannot be used to test the assumptions behind them.

**4.3. Proton Hydration Free Energy.** As discussed above, once the absolute solvation free energy of a single ion is resolved, all remaining ions can be determined as well, because the relative solvation free energies are well known. As a result, ionic solvation free energies are often reported as conventional values, relative to the solvation free energy of the proton.<sup>113</sup> This has focused a great deal of attention on accurately determining the exact value of this quantity.<sup>10,24,38,42,51,52,54,114</sup>

Table 8 summarizes H<sup>+</sup> and OH<sup>-</sup> solvation free energies from a selection of values reported in the literature. It is immediately apparent that despite a spread of almost 15 kcal/mol in proton

hydration values, the sums for the neutral H<sup>+</sup> + OH<sup>-</sup> pair are quite consistent with the exception of that given by Marcus.<sup>114</sup> The hydroxide value from Friedman and Krishnan<sup>24</sup> appears to be an outlier inconsistent with the rest of their data; values derived from their chloride or bromide free energies combined with the conventional free energy differences relative to the proton are consistent with other data sets.<sup>113</sup> Indeed, the experimental data in the first three columns of Table 8 are consistent to within 0.3 kcal/mol.

Of the theoretical predictions, two involve the use quantum mechanical representations of the solute ion along with a small number of water molecules. The effects of the bulk solvent are included using a dielectric continuum. The calculated values from Asthağiri et al.<sup>45</sup> do not reproduce the free energy of solvation for the neutral pair H<sup>+</sup> + OH<sup>-</sup>, while those from Zhan and Dixon are in excellent agreement with the experimental value for the neutral pair.<sup>52,53</sup> The two calculations differ primarily in two respects. First, Zhan and Dixon use larger basis sets and perform an extrapolation to the frozen core CBS limit. Second, different models are used to calculate the electrostatic interactions between the ion–water clusters and the surrounding dielectric. Asthağiri et al. performed the continuum calculations using atomic partial charges assigned on the basis of their quantum calculations, while Zhan and Dixon performed self-consistent reaction field calculations which include polarization of the cluster by the surrounding continuum.

The known free energy differences between K<sup>+</sup> and H<sup>+</sup> and between Cl<sup>-</sup> and OH<sup>-</sup> were used to translate the AMOEBA simulation results into predictions for the proton and hydroxide. The resulting value for the neutral H<sup>+</sup> + OH<sup>-</sup> pair is -367.4 kcal/mol, which differs by about 0.5 kcal/mol from the experiment. This error is only slightly larger than that of Zhan and Dixon. However, the two methods disagree as to the solvation free energies for the individual ions by roughly 10 kcal/mol. Both methods constitute ab initio predictions of the solvation free energies. There is only one empirical parameter in the work of Zhan and Dixon, which was determined prior to the study.<sup>52</sup> Similarly, the AMOEBA force field parameters for water and formamide were determined prior to this work, while the ion parameters were chosen to match quantum and experimental results on ion–water dimers (see section 2, Methods), without reference to the liquid phase.

One possible cause for the discrepancy is the absence of the phase potential in the calculations of Zhan and Dixon.<sup>52,53</sup> As discussed by Ashbaugh,<sup>44</sup> creating an empty sphere in water induces a positive electrostatic potential at the center of the

(113) Fawcett, W. R. *J. Phys. Chem. B* **1999**, *103*, 11181.(114) Marcus, Y. *J. Chem. Soc., Faraday Trans.* **1991**, *87*, 2995.

sphere. This potential does not go to zero as the sphere grows, but rather converges to the surface potential of an air–water interface. The effect, due to preferential orientation of water molecules at the liquid surface, is not present in a continuum model, such as that used by Zhan and Dixon.<sup>45</sup> Ashbaugh's work using classical three-site nonpolarizable water models indicates that this potential could be roughly +5–10 kcal/(mol e).<sup>44</sup> This would increase the favorability of solvating a monovalent cation by 5–10 kcal/mol and decrease that of an anion by a similar amount, without significantly altering the sum. While the estimate from the study by Ashbaugh may not be quantitatively accurate due to limitations in the water model used, it does appear that inclusion of this term would greatly diminish the difference between the quantum mechanical results of Zhan and Dixon and the results presented here.

In all likelihood, the AMOEBA ion parameters could be altered such that the Zhan and Dixon proton and hydroxide hydration values are reproduced. However, doing so would greatly degrade the structural and energetic properties of the ion–water dimers shown in Table 2. Using perturbation analysis, we estimate that for every 1 kcal/mol shift in the free energy of solvation, the interaction energy of the gas phase shifts by about 1/3 kcal/mol. Thus, altering the  $K^+$  parameters to match the Zhan and Dixon results would likely change the gas-phase interaction energy by more than 3 kcal/mol. This means that our model cannot simultaneously reproduce the solvation energies of Zhan and Dixon and the gas-phase ion–water dimer results of Feller et al.<sup>46</sup>

## 5. Conclusions

The determination of ion solvation thermodynamics is important for a variety of problems in physical chemistry and biochemistry. However, the quantity of greatest interest, the solvation free energy for individual ionic species, cannot be determined directly from experiment without the application of an additional extrathermodynamic assumption. The standard molecular mechanics force fields cannot be used to resolve this dilemma, because they typically use the ionic solvation free energies as a benchmark for parametrization purposes. However, the AMOEBA polarizable multipole force field is sufficiently flexible that parameters developed to match gas-phase *ab initio* and experimental results accurately describe the ion energetics in multiple solvents. Free energy calculations using this force field match experimental whole salt solvation and transfer results very well. As these quantities are determined experimentally, without reference to extrathermodynamic assumptions, they are more reliable than the single ionic solvation values. In fact, on the basis of the current results, we suggest that our simulations, which differ by several kilocalories from values found in the literature, are the best available estimate for the single ion solvation free energies.

**Acknowledgment.** We would like to thank Dr. H. S. Ashbaugh and Dr. R. V. Pappu for helpful conversations. This work was supported in part by NSF Award 9808317 to J.W.P. and NIH NRSA fellowship 5F32NS042975 to A.G.

JA037005R